Journal of Catalysis **191,** 55–61 (2000)
doi:10.1006/jcat.1999.2799, available online at http://www.idealibrary.com on IDEAL®

Origin of First-Order Kinetics during the Bimolecular Cracking of *n*-Hexane over H-ZSM-5 and H-β Zeolites[1]

Stefan Kotrel, Michael P. Rosynek, and Jack H. Lunsford[2]

Department of Chemistry, Texas A&M University, College Station, Texas 77843

Received July 6, 1999; revised November 8, 1999; accepted November 17, 1999

An *in situ* diffuse reflectance infrared Fourier-transform spectroscopy (DRIFTS) study of *n*-hexane cracking over H-ZSM-5 and H-β zeolites has been carried out to elucidate the origin of first-order kinetics under bimolecular conditions. Contrary to an earlier proposal, the acidic protons are not extensively complexed with olefins during reaction. A simple qualitative kinetic model that consists of six elementary reactions has been used to rationalize the first-order rate law for *n*-hexane conversion with only a small fraction of the protons being complexed. Because of competing reactions, the olefin concentration, and, hence, the protonated-complex concentration, apparently becomes constant as a function of residence time and is independent of the hexane concentration.

INTRODUCTION

Haag and co-workers (1, 2) have proposed that the acid-catalyzed cracking of simple paraffins occurs by both a unimolecular mechanism and bimolecular mechanism and that the reaction conditions can be adjusted to favor one or the other of these mechanisms. In the unimolecular mechanism, an acidic proton reacts with a paraffin molecule to form a pentacoordinated carbonium ion intermediate, which, according to computational results, may only exist in a transition state (3, 4). The bimolecular mechanism, also known as the classic mechanism, involves the formation of an alkoxide ion as a result of the reaction between an acidic proton and an olefin. The alkoxide ion, which is a true intermediate, then reacts with a paraffin molecule to produce another paraffin molecule and a new alkoxide ion. The alkoxide ions may isomerize prior to reacting with the paraffin.

Olefins are obviously required for the bimolecular reaction, and they are believed to be formed via the unimolecular reaction. Conditions that favor a larger olefin concentration in the catalyst bed, such as a longer residence time and an increased level of conversion, result in an increasing contribution of the bimolecular mechanism to the overall catalytic reaction. In a conventional plug flow reactor, unimolecular reactions might dominate in the initial section of the bed and bimolecular reactions could prevail in the final section, depending on the partial pressure of the paraffin, the residence time, and the temperature of reaction.

A rate law that includes both processes may be written as (2)

$$r_{\text{cracking}} = r_{\text{uni}} + r_{\text{bimol}} = k_{\text{uni}}[\text{RH}](1-\theta) + k_{\text{bimol}}[\text{RH}]\theta, \quad [1]$$

where [RH] is the concentration of the paraffin on/in the catalyst and θ is the fraction of Brønsted acid sites complexed with olefins. It is generally assumed that the complexation obeys a Langmuir isotherm such that

$$\theta = \frac{K[\text{Ol}]}{1 + K[\text{Ol}]} \qquad [2]$$

where K is the adsorption equilibrium constant or the equilibrium constant for the complexation (i.e., to form the alkoxide ion), and [Ol] is the olefin concentration.

If the olefin concentration is very small or if the reaction is carried out at high temperatures so that K is small, the value of θ will be small, and the rate will be dominated by r_{uni}. Conversely, at moderate olefin concentrations and at lower temperatures it has been suggested that θ approaches unity and the rate is dominated by r_{bimol}. We have shown that for the cracking of *n*-hexane over H-ZSM-5 and H-β zeolites k_{bimol} is about an order of magnitude greater than k_{uni} (5).

Under conditions such that the unimolecular mechanism prevails, first-order kinetics with respect to hexane are observed as expected from Eq. [1]. But under bimolecular conditions, first-order kinetics are also observed, and the reason for this is not so obvious since θ is a complex function of the olefin concentration (Eq. [2]) which, in turn, depends on a number of factors, including the concentration of the paraffin. In an effort to explain the first-order kinetics under bimolecular conditions, Haag *et al.* (2) proposed that most of the protons are involved in alkoxide ion formation and θ approaches unity. Thus, the first-order rate

---

[1] In memory of Werner Haag (1926–1998).

[2] To whom correspondence should be addressed.

0021-9517/00 $35.00

law

$$\lim_{\theta \to 1} r_{\text{cracking}} = k_{\text{bimol}}[\text{RH}] \qquad [3]$$

would result.

In the foregoing discussion, it has been assumed that the olefin complex is an alkoxide ion, although the olefin may also be bound to the proton as a moderately stable π complex (4). Furthermore, in the literature, the olefin complex is referred to as a carbenium ion. Computational models indicate, however, that this fully protonated adduct exists on the surface only in the transition state, and, as noted above, it is more appropriate to view the true surface intermediate as an alkoxide ion.

The purpose of the study described here was to determine whether the acidic protons in H-ZSM-5 and H-β zeolites are indeed extensively complexed during the cracking of *n*-hexane under bimolecular conditions. *In situ* diffuse-reflectance infrared Fourier-transform spectroscopy (DRIFTS) was used to follow the concentration of surface OH groups and other species during reaction.

EXPERIMENTAL

H-β (PQ,CP-811A1-25) and H-ZSM-5 (PQ, CBV 5020 E) zeolites were transformed into their ammonium forms by ion exchange. Approximately 20 g of zeolite was exchanged six times in 500 mL of 1 M NH_4NO_3 for 8 h at 358 K. The zeolites were pretreated by heating them *in situ* in flowing dry N_2 at 373, 473, 573, and 673 K for 1 h at each step. Between steps the heating rate was 5 K min^{-1}. The residual sodium contents and the Si/Al ratios, as well as the concentrations of acid sites, have been reported previously (5, 6). For H-β and H-ZSM-5, Si/Al ratios were 16.6 and 35.0, respectively, for which only the amount of framework aluminum was considered. The corresponding concentrations of acidic protons were 0.93 and 0.46 mmol/g.

The *n*-hexane cracking reactions were carried out in the *in situ* DRIFTS cell described below and in conventional plug flow reactors. The latter consisted of fused-quartz tubes with an internal diameter of 3, 4, or 6 mm, depending on the catalyst volume. A stream of N_2 (65 mL min^{-1}) was passed through an *n*-hexane (99+%, Janssen Chemica) saturator and, when necessary, was diluted with pure N_2 before it was allowed to enter the reactor. Rate and selectivity data were obtained mainly at an *n*-hexane partial pressure of 5.3 kPa, but some results were obtained at 0.25 kPa. The reaction products were sampled with an eight-port valve and subsequently analyzed by gas chromatography (Hewlett–Packard Model 5890) with an Al_2O_3/KCl-coated fused-silica capillary column. Additional details on the method used to determine the reaction rates in the plug flow reactor are given in Ref. (5).

The *in situ* infrared and catalytic measurements were carried out at 623 K with a Perkin–Elmer Spectrum 2000 spectrometer equipped with an MCT detector and a DRIFTS cell (Harrick) used in the flow mode. The reactor part of the cell consisted of a temperature-controlled metal cup in which the catalyst powder was loosely packed and through which the feed gas was allowed to flow. An undiluted zeolite sample was placed in the DRIFTS cell and was degassed in the same manner as in the conventional catalytic reactor. The gas flow was from bottom to top, so that the DRIFTS spectra could be recorded from the exit of the catalyst bed. This is significant since the olefin concentration would be the largest at this point. Spectra were collected prior to and several times during the cracking experiment and were recorded in the ranges from 2500 to 4000 cm^{-1} and 1300 cm^{-1} to 1700 cm^{-1}. For each spectrum, results from 200 scans with a resolution of 4 cm^{-1} were collected. The spectra are reported using the Kubelka–Munk function if the absorbance was small and as arbitrary reflectance if the absorbance was large. The analytical system and the preparation of the feed gas were the same as those described above, but with the DRIFTS cell, CH_4 was used as an internal standard for the calculation of conversion and product selectivities. Methane was also a minor product, but its concentration as a standard was 50 times larger than that produced during the conversion of *n*-hexane.

KINETIC RESULTS

Conversions and product selectivities for *n*-hexane cracking in the DRIFTS reactor and in the conventional plug flow reactor are given in Table 1. The large *i*-butane and

TABLE 1

Initial Molar Selectivities (%) for *n*-Hexane Cracking at $p_{\text{Hex}} =$ 5.3 kPa and $T = 623$ K over H-ZSM-5 and H-β Zeolites

	H-ZSM-5		H-β	
	DRIFTS	Plug flow reactor	DRIFTS	Plug flow reactor
CH_4	IS[a]	0.4	IS[a]	0.06
C_2H_6	4.3	2.9	0.7	0.5
C_2H_4	11.2	6.7	4.7	1.5
C_3H_8	41.4	33.0	43.0	31.7
C_3H_6	11.5	15.6	6.5	6.3
n-C_4H_{10}	10.0	14.7	9.3	10.0
Iso-C_4H_{10}	8.8	7.3	22.2	22.7
C_4H_8	5.8	11.3	1.5	2.1
C_5H_{12}	2.8	5.1	5.1	13.3
C_5H_{10}	0.6	0.3	0.0	0.6
Iso-C_6	3.6	2.5	7.1	11.2
Contact time(ms)	60	79	29	27
Conversion (%)	15.0	14.5	29.0	22.6
P/O ratio	2.3	2.7	6.5	10.0

[a] CH_4 was used as an internal standard.

propane selectivities and the small methane and ethane selectivities together with the large paraffin-to-olefin ratio observed over the H-β zeolite are characteristic of bimolecular cracking. Thus, the spectroscopic results obtained in the DRIFTS cell are applicable to bimolecular cracking. To a smaller extent, the same trends were observed over the H-ZSM-5 zeolite, but since the conversion was less, the bimolecular mechanism may not be as fully developed (see below). As noted previously (5), the total activity of the H-β zeolite is considerably greater than that of the H-ZSM-5 zeolite, in part because of the enrichment of *n*-hexane in the pores of the former catalyst. The number of acid sites per gram of material was also larger in the H-β zeolite. The differences in the concentrations of certain components, such as the amounts of C_2H_4 produced in the two reactors, may result from the extent of backmixing, which is greater in the DRIFTS reactor.

The initial molar selectivities that are reported in Table 1 do not include oligomeric coke, aromatic coke, or volatile aromatics. Oligomerization of light olefins is known to be rapid over acidic zeolites at these temperatures (7), and such reactions would be, in part, responsible for the initial loss of C_2H_4 and C_3H_6, and consequently for P/O ratios that are greater than unity. As a result of hydrogen transfer and cyclization reactions, aromatic products, including aromatic coke, are formed. Over H-ZSM-5, volatile aromatic products are favored. Ping *et al.* (8), for example, have shown that over H-ZSM-5 at 400°C a dilute stream of ethylene (3% C_2H_4 in CH_4) is extensively converted, with 19% aromatic selectivity. In the H-β zeolite, aromatic coke formation is evident as noted below under Spectroscopic Results. These reactions provide a mechanism for the depletion of olefins. Moreover, hydrogen transfer reactions that accompany aromatic formation can yield additional paraffins.

Kinetic results obtained at 0.25 and 5.3 kPa are depicted as first-order plots in Fig. 1. The results in the high-pressure regime (Fig. 1a) are characterized by a typically slower rate (smaller slope) at shorter residence times and a faster rate (larger slope) at longer contact times (2). As noted by Haag *et al.* (2), the reaction at short residence times is essentially unimolecular because the olefin concentration is small, but at longer times the olefin concentration increases and bimolecular reactions, which have a larger rate constant, begin to dominate. Because of the higher activity of H-β, the bimolecular reaction controls the kinetic behavior even at residence times as short as 30 ms. The first-order behavior, indicated by the straight line, does not become apparent over H-ZSM-5 until about 100 ms.

Surprisingly, even at the lower pressure, first-order behavior was not strictly obeyed over the H-β zeolite as shown in Fig. 1b. At shorter residence times the cracking was truly unimolecular, but at longer residence times, as more olefins were formed, the more rapid bimolecular reaction began to contribute to the conversion. Over H-ZSM-5, the conversion was less and the reaction was first order over the entire range of residence times.

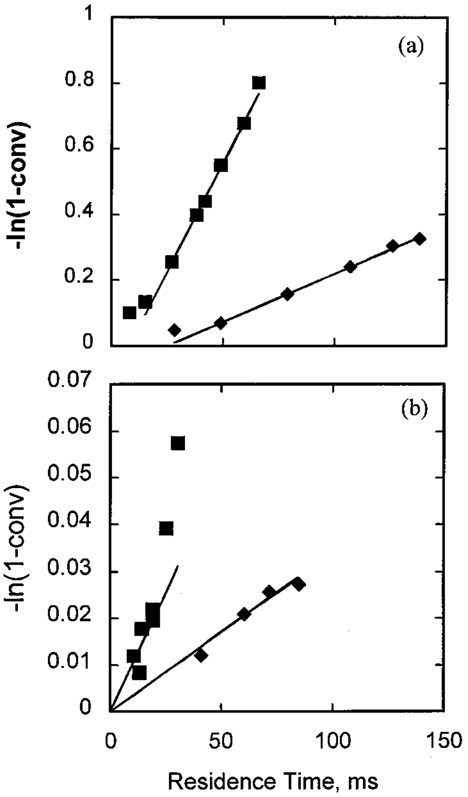

FIG. 1. First-order plots for *n*-hexane cracking at (a) 5.3 kPa and (b) 0.25 kPa over (■) H-β and (◆) H-ZSM-5. The solid lines indicate the regions of first-order behavior.

SPECTROSCOPIC RESULTS

The variations in the $\nu(OH)_{stretch}$ bands for H-ZSM-5 and H-β zeolites prior to and during the *n*-hexane cracking are shown in Fig. 2. There is a considerable red shift of all $\nu(OH)_{stretch}$ bands at elevated temperatures with respect to the positions of the bands at lower temperatures (9). For H-β zeolite, four types of OH groups can be distinguished, and for H-ZSM-5 zeolite three types can be distinguished. The band at 3594–3597 cm^{-1} is assigned to acidic (Si–OH–Al) groups, the bands at about 3650 and 3770 cm^{-1} (not present in H-ZSM-5) are assigned to Al–OH groups associated with extraframework aluminum, and the band at 3730–3743 cm^{-1} is assigned to silanol groups.

Most importantly, the $\nu(OH)_{stretch}$ band intensities, particularly those of the Brønsted acid centers, did not decrease substantially on exposure to *n*-hexane, which is contrary to the results expected from the kinetic model of Haag *et al.* (2). The amplitudes of the Si–OH–Al band and the *n*-hexane conversions for both zeolites are shown in Fig. 3 as

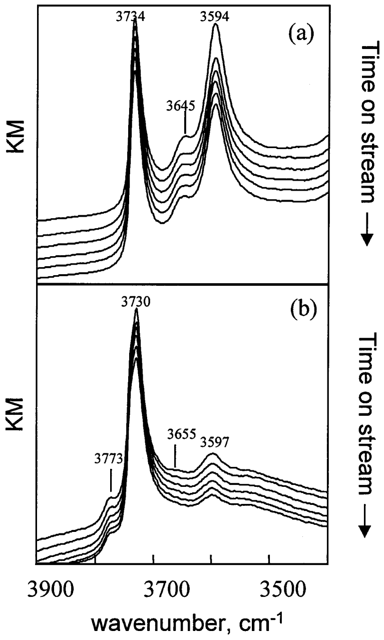

FIG. 2. *In situ* DRIFTS during *n*-hexane cracking at 623 K and $p_{\mathrm{Hex}} =$ 5.3 kPa: (a) H-ZSM-5 after 0, 4, 12, 30, 37, and 48 min on stream and (b) H-β after 0, 5, 17, 30, 43, and 62 min on stream.

a function of time on stream. A rapid decrease of 10–20% in the IR band intensities was followed by either a constant intensity for H-ZSM-5 zeolite or a continuous slow decrease for H-β zeolite. Had the acidic protons been extensively complexed with the olefinic products, one would have expected the acidic OH bands either to significantly shift in frequency (see below) or to decrease in amplitude to very low values. Obviously, neither of these results occurred. It is conceivable that only a small subset of the observed Si–OH–Al centers are active in catalysis, but Na^+ poisoning experiments with these same materials indicated that about 80% of the acidic hydroxyl groups are involved (6).

The strong infrared bands at 2874, 2935, and 2964 cm^{-1} in Fig. 4a indicate the presence of physisorbed *n*-hexane and other hydrocarbons in the zeolite under reaction conditions. About one-third of the amplitude corresponds to *n*-hexane in the gas phase. The spectrum with the smallest amplitude was recorded after 4 min exposure, and the remaining three were recorded after 12, 30, and 48 min, respectively. As previously demonstrated, H-ZSM-5 zeolite would have 1.64 mmol/g of hexane in its channels at 623 K and 5.3 kPa (5). The amplitude of the band at 3595 cm^{-1} decreased slightly, but this was probably a result of increasing *n*-hexane pressure and increasing time on stream (see Fig. 2). It is significant that only a small increase in absorbance was noted at ca. 3500 cm^{-1} which indicates the presence of very little hydrogen-bonded hexane. The weak bands at ca. 3200 cm^{-1} may result from a π complex between Brønsted acid centers and light olefins (10), but again, only a small fraction of the protons is involved. This behavior is in contrast to that indicated by the spectral changes depicted in Fig. 4b for *n*-hexane adsorption on H-ZSM-5 at 453 K. At this lower temperature, there is clear evidence for extensive hydrogen bonding as indicated by the large decrease in OH bands at 3602 and 3656 cm^{-1} and a concomitant increase in the band at 3490 cm^{-1} as the *n*-hexane pressure was increased to 1.3 kPa. The band at 3490 cm^{-1} is due to an OH stretching mode that is perturbed by hydrogen bonding (11). This manifestation of hydrogen bonding at the lower temperatures confirms that the interactions between zeolitic protons with hydrocarbons could have been detected under reaction conditions had they involved a significant fraction of the protons.

In the region 1300–1700 cm^{-1}, weak spectra due to hydrocarbon species were observed in the presence of a large absorption background as shown in Fig. 4. With H-ZSM-5, bands due to symmetric and asymmetric $\nu(\mathrm{CH})_\delta$ vibrations are present at 1380 and 1460 cm^{-1}, but with H-β only the band at 1460 cm^{-1} is evident. The intense overtones of the zeolite framework partially obscured the spectral region below 1500 cm^{-1}. New bands appeared at 1510 and 1590 cm^{-1} during the cracking reaction over H-ZSM-5 (Fig. 5a). Similar spectral features were observed for H-β (Fig. 5b), but the relative amplitudes were different. The band at 1510 cm^{-1} was small compared with that in H-ZSM-5, and a much more intense signal at 1590 cm^{-1} dominated the spectrum. The latter band increased continuously with increasing

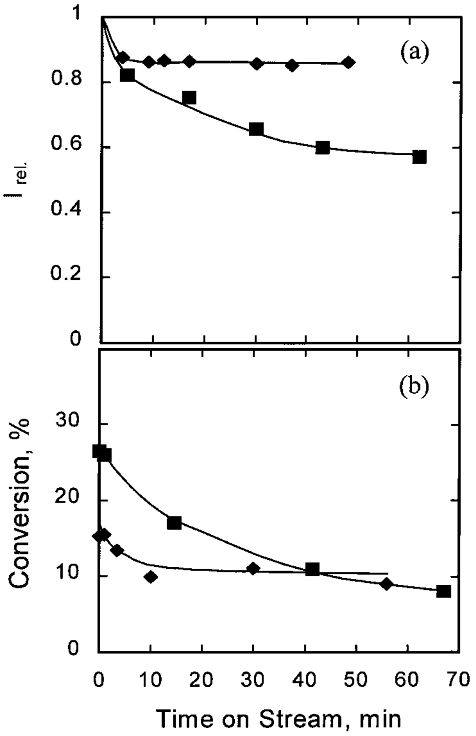

FIG. 3. Comparison of (a) the relative intensity of the ν(Si–Al(OH)–Si) stretching mode and (b) the catalytic activity for (◆) H-ZSM-5 and (■) H-β at $p_{\mathrm{Hex}} = 5.3$ kPa and $T = 623$ K as a function of time on stream.

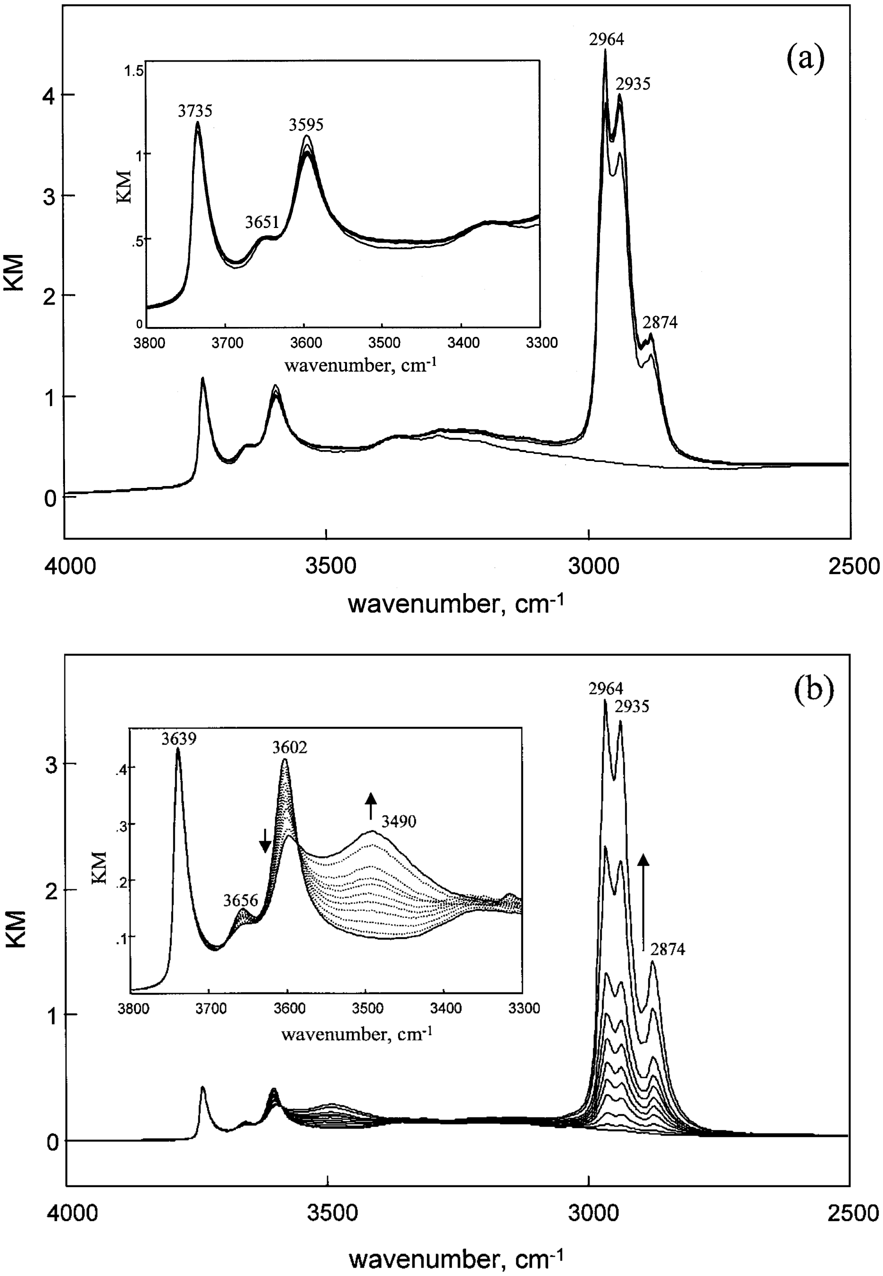

FIG. 4. *In situ* DRIFTS following the addition of *n*-hexane to the H-ZSM-5 zeolite: (a) at $p_{\mathrm{Hex}} = 5.3$ kPa and $T = 623$ K after 4, 12, 30, and 48 min; (b) at $T = 453$ K at 0.0, 0.05, 0.11, 0.18, 0.26, 0.34, 0.45, 0.53, 0.69, 0.93, and 1.3 kPa.

time on stream. When the H-ZSM-5 sample was purged with N_2, the $\nu(\mathrm{CH})_\delta$ bands at 1460 and 1380 cm^{-1} rapidly disappeared. The band at 1510 cm^{-1} remained even after the sample had been purged for 8 min, as shown in Fig. 5a, but after 20 min only a broad band at 1590 cm^{-1} remained. Similarly, the species responsible for the band at 1590 cm^{-1} was irreversibly absorbed on H-β zeolite (Fig. 5b).

The temporal behavior of the bands indicates that the spectrum at 1590 cm^{-1} is due to coke (12). Further support for this assignment was found in the color of the samples after reaction. The H-β zeolite sample, which exhibited a much larger band at 1590 cm^{-1}, was black, whereas H-ZSM-5 zeolite remained white. Similarly, in the plug flow experiments there was a small, but continuing loss of products in H-β zeolite, and, as a consequence, there was not a mass balance when coke was excluded. The slow buildup of coke, particularly in H-β, correlates well with the partial decrease in acidic hydroxyl band intensity as shown in Fig. 3b.

The origin of the band at 1510 cm^{-1} is not certain, although Lavalley (13) suggests that a cyclic carbenium ion may give rise to a signal at this wavenumber. The NMR

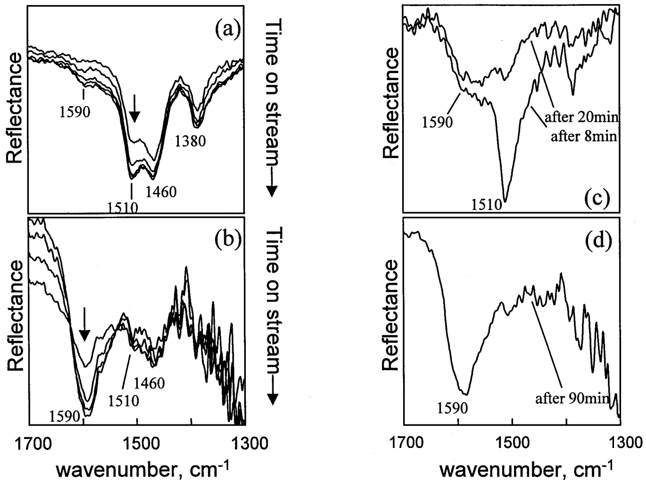

FIG. 5. *In situ* DRIFTS during *n*-hexane cracking over (a) H-ZSM-5 after 5, 12, 25, 41, and 92 min on stream and (b) H-β after 5, 25, 40, and 80 min on stream at 623 K and $p_{\mathrm{Hex}} = 5.3$ kPa; after (c) H-ZSM-5 and (d) H-β were purged with N_2.

spectrum of a methyl-substituted cyclopentyl cation was recently identified in H-ZSM-5 by Haw and Xu (14), and it has been suggested that the carbenium ion may be involved in coke formation (15). The band position also is consistent with $\nu(\mathrm{C{=}C})_{\mathrm{stretch}}$ of a substituted aromatic compound with a relatively high symmetry, such as *p*-xylene, which also may result in coke formation. In agreement with previous investigators, the band at 1510 cm^{-1} is tentatively assigned to a cyclic coke precursor. The bands at 1380 and 1460 cm^{-1} are assigned mainly to unreacted *n*-hexane, which is weakly bound in the zeolite, but other reversibly held hydrocarbon species may contribute to the spectrum.

DISCUSSION

Clearly, the acidic protons are not extensively complexed with olefins under reaction conditions, as would be required by the hypothesis of Haag *et al.* to explain first-order kinetics for a bimolecular reaction. One might argue that only a subset of the Brønsted sites are actually involved in catalysis; however, we have previously used Na$^+$ poisoning experiments to demonstrate that essentially all of the acidic protons in these two zeolites are involved in catalysis (6). This result is consistent with those of Haag *et al.* (16), who demonstrated a linear relationship between *n*-hexane cracking activity under unimolecular conditions and framework aluminum content over several orders of magnitude. In this experiment, the H$^+$/Al ratio presumably was unity.

TABLE 2

Reaction Pathways for the Model of Bimolecular *n*-hexane Cracking

Cracking reactions	
I	$P + HZ \rightarrow oHZ + p$
II	$P + oHZ \rightarrow oHZ + p$
Olefin adsorption/desorption reactions	
III	$o + HZ \rightarrow oHZ$
IV	$oHZ \rightarrow HZ + o$
β-Scission/oligomerization reactions	
V	$oHZ \rightarrow oHZ + o$
VI	$o + oHZ \rightarrow oHZ$

Since Brønsted sites are not saturated with olefins, one must seek another explanation for the first-order kinetics under bimolecular conditions. A simple model that is based on the six generic reactions given in Table 2 may be used to rationalize the results. Reactions I and II describe unimolecular and bimolecular cracking reactions, respectively. The olefin that is protonated on the zeolite obviously is different from the olefin that is a product of Reaction II; however, in the model, no distinction is made between the two olefins. Reactions III and IV describe olefin adsorption and desorption, while reactions V and VI denote β-scission and oligomerization. It is assumed that the adsorption of the olefin results directly in the formation of an alkoxide ion. The importance of oligomerization in coke formation has recently been emphasized by Williams *et al.* (17).

At a sufficiently long residence time, which is probably on the order of a 100 ms, the concentration of the complexed olefin, oHZ, will reach steady state because of competing formation and removal reactions. This concentration is small because the rate of complex removal via reactions II and IV is large compared with its rate of formation via reactions I and III. Moreover, by considering a reasonable set of rates for olefin adsorption/desorption, β-scission, and oligomerization, together with known rates for the unimolecular cracking reaction, it is possible to show that the alkoxide (oHZ) concentration is independent of *n*-hexane concentration. Thus, first-order kinetics may be observed even when the cracking reaction is bimolecular. A numerical model based on these reactions has been described elsewhere (18).

SUMMARY

Infrared spectroscopic results for H-β and H-ZSM-5 zeolites confirm that acidic protons are not extensively complexed with olefins under conditions such that bimolecular reactions dominate in the cracking of *n*-hexane and the reaction is first order. This observation is in disagreement with the usual explanation for first-order kinetics which assumes that the reaction rate depends only on the paraffin concentration because the protons are almost completely complexed with olefins. That is, the alkoxide ion concentration is independent of the paraffin concentration.

A simple kinetic model provides a plausible explanation that is consistent with the kinetic and infrared results.

Namely, by considering a set of reactions that include olefin adsorption/desorption, as well as β-scission and oligomerization, it is possible to conclude that the alkoxide concentration may be nearly independent of *n*-hexane concentration, even when most of the protons remain uncomplexed. Thus, during bimolecular cracking, first-order kinetics may prevail.

ACKNOWLEDGMENT

This work was supported by the National Science Foundation under Grant CHE-9520806.

REFERENCES

1. Haag, W. O., and Dessau, R. M., *in* "Proceedings, 8th International Congress on Catalysis, Berlin, 1984," Vol. II, p. 305. Dechema, Frankfurt-am-Main, 1984.
2. Haag, W. O., Dessau, R. M., and Lago, R. M., *Stud. Surf. Sci. Catal.* **60**, 255 (1991).
3. Rigby, A. M., Kramer, G. J., and van Santen, R. A., *J. Catal.* **170**, 1 (1997).
4. Natal-Santiago, M. A., Alcalá, R., and Dumesic, J. A., *J. Catal.* **181**, 124 (1999).
5. Kotrel, S., Rosynek, M. P., and Lunsford, J. H., *J. Phys. Chem. B* **103**, 818 (1999).
6. Kotrel, S., Rosynek, M. P., and Lunsford, J. H., *J. Catal.* **182**, 278 (1999).
7. Chang, C. D., and Silvestri, A. J., *J. Catal.* **47**, 249 (1977); Sun, Y., Campbell, S. M., Lunsford, J. H., Lewis, G. E., Palke, D., and Tau, L.-M., *J. Catal.* **143**, 32 (1993).
8. Ping, Q., Lunsford, J. H., and Rosynek, M. P., *Catal. Lett.* **52**, 37 (1998).
9. Peuker, Ch., *J. Mol. Struct.* **349**, 317 (1995).
10. Spoto, G., Bordiga, S., Ricchiardi, G., Scarano, D., Zecchina, A., and Borello, E., *J. Chem. Soc. Faraday Trans.* **90**, 2827 (1994).
11. Eder, F., Stockenhuber, M., and Lercher, J. A., *J. Phys. Chem. B.* **101**, 5414 (1997).
12. Datka, J., Sarbak, Z., and Eischens, R. P., *J. Catal.* **145**, 544 (1994).
13. Lavalley, J. C., personal communication.
14. Haw, J. F., and Xu, T., *Adv. Catal.* **42**, 115 (1998).
15. Xu, T., and Haw, J. F., *J. Am. Chem. Soc.* **116**, 7753 (1994).
16. Haag, W. O., Lago, R. M., and Weisz, P. B., *Nature* **309**, 589 (1984).
17. Williams, B. A., Babitz, S. M., Miller, J. T., Snurr, R. Q., and Kung, H. H., *Appl. Catal. A* **177**, 161 (1999).
18. Kotrel, S., Ph.D. thesis, University of Munich, 1999.